A Report on

Dynamics of weakly bound projectile induced reactions using fragmentation approach

Submitted towards the partial fulfilment for the requirement of the degree of

Master degree in Physics

Submitted by

Shilakha Dawar

Roll No-301304008

Under the supervision of

Dr. Manoj K. Sharma
Professor & Head of Department

School of Physics and Material Science

Thapar University, Patiala – 147004

July 2015

I dedicate this thesis to my family

CERTIFICATE

I hereby certify that the work which has been presented in this thesis entitled, "**Dynamics of weakly bound projectile induced reactions using fragmentation approach**" submitted for partial fulfilment of the requirements for the award of degree of **Masters of Science** in **Physics** at **Thapar University, Patiala,** is an authentic record of my own work carried out under the supervision of **Dr. Manoj K. Sharma, Professor & Head, SPMS** and refers other researcher's work which are duly listed in reference section.

The matter embodied in this thesis has not been submitted for the award of any other degree of this or any other university.

Shilakha Dawar

Date: 14 July 2015 (Shilakha Dawar)

This is to certify that the above statement made by the candidate is correct and true to best of my knowledge.

Dr. Manoj K. Sharma
Professor and Head of Deptt.
SPMS, Thapar University

Countersigned By:
Dr. Manoj K. Sharma
Professor and Head of Deptt.
SPMS, Thapar University

Dr. S.S. Bhatia
Dean of Academic affairs
Thapar university

Acknowledgement

I would like to thank all the people who contributed in some way to the work described in this thesis. First and Foremost, I would like to express my sincere gratitude to **Dr. Manoj K. Sharma**, my worthy supervisor, **Professor and Head of School of Physics and Material Scienc**e. Without him the dissertation would not have been viable. I thank him for his patience, motivation, enthusiasm, and immense knowledge. His guidance helped me in all the time of research and inscribing of this Dissertation. I could not have imagined having a better advisor and mentor for my Masters Degree Dissertation. I express my sincere thanks to him for his valuable enlightenment in carrying out this work under his effectual supervision, encouragement and co-operation. His visionary thoughts have influenced me profoundly. His dynamical attitude has empowered me with zeal of energy to conquer the minor details of my research work.

Every result described in this thesis was accomplished with the help and support of fellow lab mates. My sincere thanks also goes to **Ms. Neha Grover**, research Scholar for the help and valuable suggestions provided by her. I greatly benefited from her keen scientific insight, her knack for solving seemingly intractable difficulties, and her ability to put complex ideas into simple terms. I gained a lot from her vast physics knowledge and scientific curiosity. I owe a debt of gratitude to all the members of the Nuclear Theory Lab for all the valuable guidance all through this effort. I thoroughly enjoyed each and every one of them and learned so much from their "exercise wisdom" that I could share within my work.

Special thanks to all my friends and the staff at the School of Physics and Material Science for providing me a friendly atmosphere and encouraging me round the slog.

Last but not the least I would like to express my heart-felt gratitude to my family for the unceasing encouragement, support and attention. Their upright support has bared fruit through completion of this thesis.

I also place on record, my sense of gratitude to one and all who directly or indirectly, have lemt their hand in this venture.

Patiala

July, 2015

Shilakha Dawar

5

Contents

List of figures

List of Tables:

Abstract

The current wave of interest is, understanding the structure and dominant reaction mechanism of loosely bound nuclei or one can say that the nuclei far from stability. Reactions induced with loosely bound nuclei are substantial as in these reactions, the processes apart from complete fusion (CF) and transfer reactions can be observed. Many other processes such as incomplete fusion, quasi fission, and deep inelastic collision may also be observed. Hence the advantage of studying such reactions is that the effect of loosely bound nuclei on fusion and consequently on the decay of the compound nucleus can be explored, which in turn provides deeper insight of associated aspects. In this work, we have investigated the decay of $^{217}Rn^{*}$ and $^{218}Fr^{*}$ nuclei formed respectively in $^{9}Be + ^{208}Pb$ and $^{9}Be + ^{209}Bi$ reactions. All calculations have been done within dynamical cluster decay model (DCM) framework in reference to the experimental data of 2010. In order to deal with the experimental data, one needs to have heedful insight into various extremities like excitation energy, angular momentum and temperature etc. Interestingly, DCM with all these features included into it, imparts information for the decay patterns of the nuclear systems formed in heavy ion reactions. The study of decay of given compound nuclei have been carried out by taking quadrupole deformations (β_2) i.e. prolate and oblate, and the two possibilities of decay have been observed i.e. evaporation residue and fission, whereas fission contribution is found to be negligibly small as compared to evaporation residue. Further, as ^{9}Be being loosely bound nuclei may disintegrate into ^{5}He and ^{4}He as given in experimental data, this weakly bound characteristic of ^{9}Be may lead to the fusion of either ^{5}He or ^{4}He with respective targets, leading to incomplete fusion. Thus the decay study of incomplete fusion has also been carried out in terms of evaporation residue production in framework of DCM.

Chapter I

Literature Review

Chapter-I

1.1 Introduction

Searching for the furthest building blocks of the corporeal world has always been a central theme in the antiquity of scientific research. This pursuit had its beginning in the speculations of early Greek philosophers. In fourth Century BC the notion of atomism to full-fledged atomic theory was instigated by "Democritus". Evidently, the next step was to uncover the modules of this basic constituent of matter which led to the origin of nuclear physics from Becquerel's discovery of radioactivity in 1896. Subsequently, Rutherford's hypothesis established the existence of nucleus in 1911 to the contrivance of four fundamental forces. It is clear that nuclear science have played a prominent role in the build out of physics arena till date. In spite of tremendous amount of information available about the atomic nuclei, nuclear physics is still treated as a young subject with lot of promises in its store. Nuclear physics research seeks answer to questions regarding the evolution of universe preceding the evolution of Big Bang from the super-hot plasma, and how different elements existing were formed, with their nucleus comprising of individual protons and neutrons interacting with each other. The understanding of atoms and molecules and their interactions has led to practical advances in almost every sphere of human endeavour. Fundamental studies in nuclear sciences have been continuously providing the basis for functional applications at an ever increasing rate.

Advancements in technology stimulated by the demands of nuclear research have led forthwith to the modelling of the research and analytical tools in the fields ranging from environmental to medicinal science extending to art and archaeology as well. These new technologies also give rise to the practical applications stretching from integrated circuit production to weapons verification. From future perspective the emerging applications of nuclear technology indicates to fulfil numerous future needs of the human kind.

Also, the properties of nuclei can be studied in terms of various mathematical models exhibiting information about nuclear structure and the internal motion. Various

nuclear models were propounded to study the properties of nuclei and structure effects associated with them. Whether it be the liquid drop model elucidating numerous properties of nuclei together with the general trend of binding energy with respect to mass number, and the phenomenon of nuclear fission, or it be the shell model unfolding the drawbacks of liquid drop model, giving rise to revelation of magic numbers and spherical symmetry of nucleus, each model endowed us with the obscured peculiarities of the beginning bud.

To include motions of the whole nucleus such as quantized rotations and vibrations unspecified by the shell model, the collective model invaded into picture as an extension of liquid drop and shell model, emphasizing typically of the coherent behaviour of all the nucleons and providing a good starting point for understanding nuclear behaviour such as fission. In addition to fission, it has been successful to a great extent in elucidating a number of nuclear properties, especially the energy levels in nuclei having even number of protons and neutrons, excited state dynamics, angular momentum, magnetic moments and nuclear shapes etc. In late 1955, a basic single-particle model applicable to deformed nuclear systems Nilsson model, was proposed by Sven Gösta Nilsson, with the work of Leo James water, Aage Bohr and Ben Mottelson. Such collective picture based nuclear models have been exploited extensively over last few decades to understand and address the nuclear reaction dynamics and related structure issues at low energy regime.

1.2 Nuclear Reactions

In contrast to the historical evolution of atomic physics, which was scrutinized by spectra of atoms by using experimental and theoretical methods, nuclear physics was explored via nuclear reactions involving compound and non compound nucleus paths using shell model as well as collective model descriptions. In order to study the properties of nuclear matter, nuclei and nucleons, nuclear reactions play an extremely eminent role. It is relevant to mention here that the understanding of the physics via nuclear reactions at low energies is crucial for explaining the numerous facts about the evolution of the Universe.

Nuclei and nuclear reactions can be foreseen as playground of three fundamental interactions in nature namely, electromagnetic interactions, strong interactions and weak interactions. A nuclear reaction can be fathomed as a collision between two nuclei that drives the change in the nuclear composition and/or the energy state of the interacting partners.

In a typical reaction, a projectile is incident on a target nucleus and after the knock a daughter nucleus and outgoing particle(s) are discerned. Nuclear reactions can be classified on the basis of numerous criteria such as energy of projectile hitting target, the energy of reactants, mass asymmetry of colliding partners, related shapes of colliders etc. For example a brief description of nuclear reactions on basis of beam energy is given below in fig 1.1

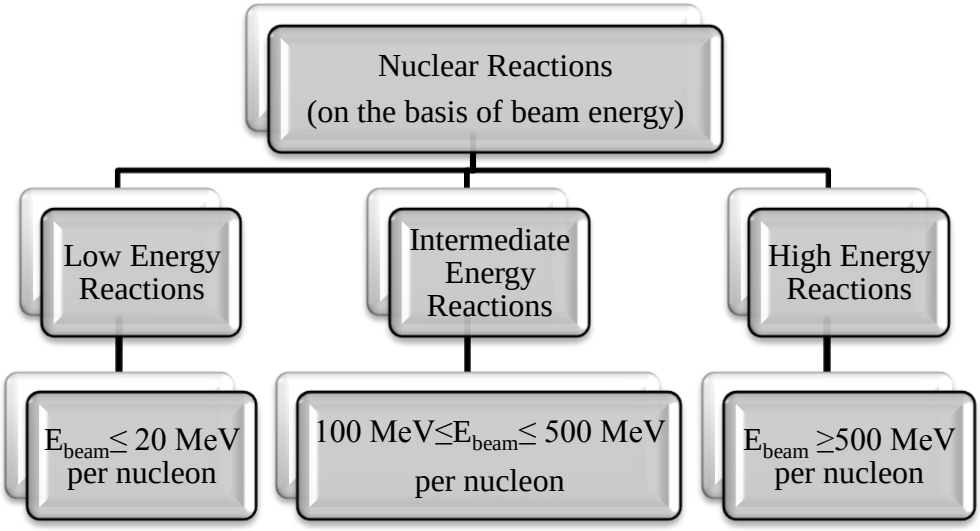

Fig 1.1: Classification of nuclear reactions on the basis of beam energy

It may be noted that, in present work, the emphasis is to address the low energy heavy ion collisions and associated dynamical aspects. Therefore the main focus will be on the low energy dynamics in the subsequent sections.

Nuclear reactions can be either exothermic or endothermic depending on the Q value. On the basis of mechanisms that governs the process (intermediate stage of colliding

nuclei), one may distinguish two extreme cases of nuclear reactions namely compound nucleus and non compound nucleus reactions as illustrated in figure 1.2.

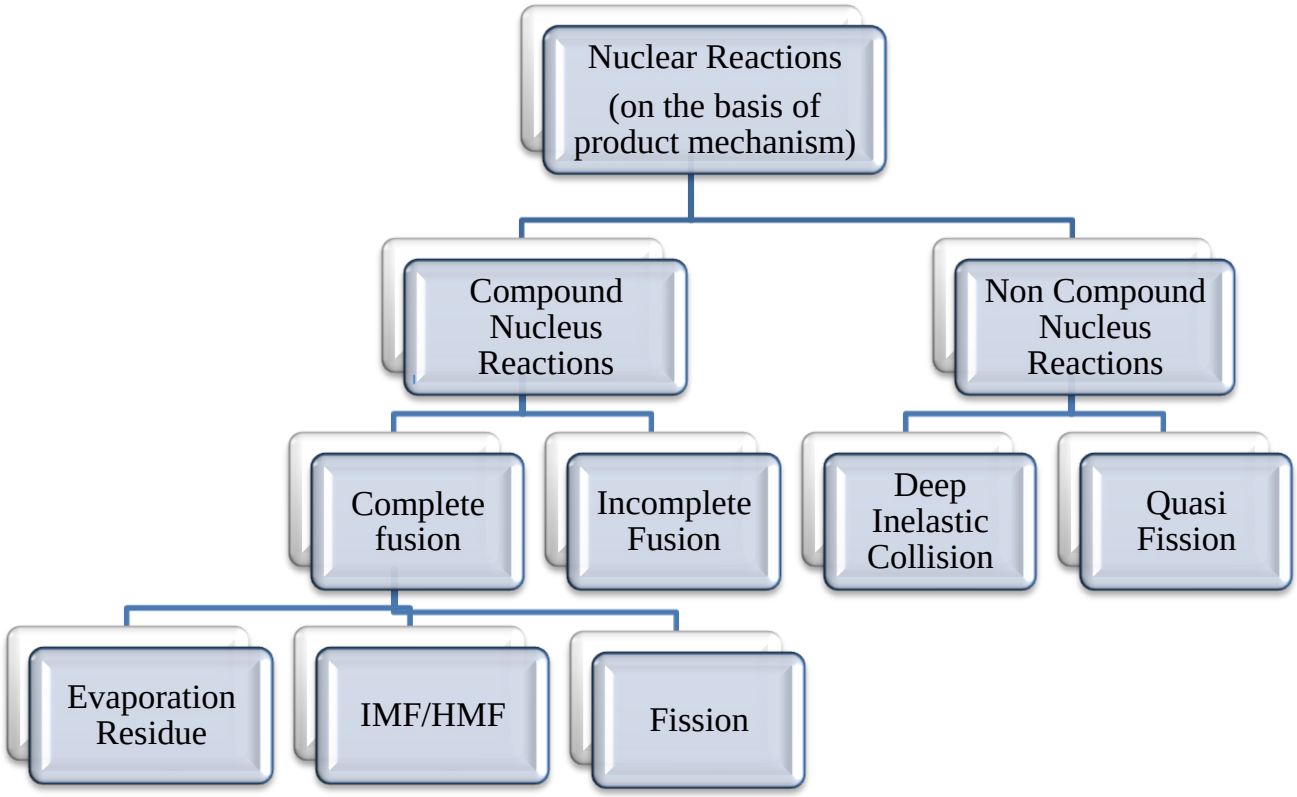

Fig1.2: Classification of nuclear reactions on the basis of product mechanisms

1.2.1 Compound Nucleus Reactions (CN)

The idea of compound nucleus entered the scenario to explain the narrow resonances observed in scattering experiments performed using low energy neutrons. The basic lay out of the theory of compound nucleus reactions was proffered by Niels Bohr in 1936. It was proposed that a nuclear reaction begins with projectile being captured by the target nucleus where after its energy is shared among all the nucleons of the compound nucleus formed. The life time of the compound nucleus ($10^{-14}s$-10^{-16}s) is long enough as compared to nuclear interaction time ($10^{-21}s$-$10^{-22}s$). During the formation of compound nucleus (CN), sharing of energy takes place almost uniformly, due to which all memory of formation channel gets generally lost.

In other words, the process of formation and decay are in general independent of each other, as affirmed by Bohr independence hypothesis [1]. The Compound nucleus reactions play an important role at low energies, and act as an apt source of information in describing the nuclear structure.

The interaction trajectories relying on impact parameters for the formation of composite system and pertinent shape of projectile nucleus, may lead eminently to reaction processes like

(i) Complete fusion (CF)
(ii) Incomplete fusion (ICF)

1.2.1.1 Complete fusion

Complete fusion between two heavy mass nuclei can be envisaged as a complete concoction of all the nucleons of the target and projectile that leads to the formation of a composite system formed inside the fission barrier. The essentiality for complete fusion reaction to occur is that the interacting nuclei must have high energy which is enough to overcome the Coulomb barrier owing to the electromagnetic repulsion between the protons [2]. However the Coulomb repulsion between the nuclei is overcome by short range but stronger attractive nuclear force which is imperative to bring the two nuclei close enough to each other in order to ensure that nuclei collide with sufficient amount of kinetic energy. In other words, fusion can also be foreseen as quantum tunnelling through the barrier formed by long range Coulomb potential, centrifugal or angular momentum potential and the proximity or short range nuclear potential [3]. Recent knowledge on collisions of strongly bound nuclei depicts that they have high breakup thresholds. However for collisions of light weakly bound nuclei with stable or deformed targets, the situation may be quite different. The breakup threshold is very low for these cases, consequently affecting the fusion process profoundly. The foremost aspect of collision of weakly bound nuclei is that fusion processes can take place in different manifestations. Direct complete fusion (DCF), being the simplest one, involves the complete assimilation of projectile by the target. Drawing the analogy, these processes are alike the fusion process of strongly

bound nuclei, where the only possible addition being the fusion following breakup. The projectile in these cases is segregated into two or more fragments as it approaches the target followed by complete or partial absorption of fragments subsequently. When all the dissociated fragments fuse with the target individually, the process is called as sequential complete fusion (SCF). However, if the projectile's fragments are only partially absorbed (at least one fragment comes up from the interaction region) the process is called incomplete fusion, ICF (discussed ahead). From experimental perspective, DCF and SCF are difficult to distinguish between.

1.2.1.2 Incomplete fusion

If the projectile breaks due to increment in energy or loosely bound structure before the collision then this partial projectile may lead to incomplete fusion. This process is generally observed when loosely bound projectile such as ^{6}Li, ^{11}B, ^{11}Be etc. are involved in reaction dynamics. In ICF reaction, the projectile is reckoned to disintegrate within the nuclear field of the target nucleus into constituent clusters, where the partial fusion of one of the clusters occurs with target to form new nuclear system having mass relatively lesser, charge and energy of excitation as compared to the compound nucleus formed in complete fusion process. As in this process there is a partial fusion of projectile, thus only fractional momentum transfer takes place.

These reactions require relatively higher value of impact parameter for collisions trajectories with $\ell > \ell_{crit}$, in which the centrifugal potential inundates attractive nuclear potential, thus the pocket in the entrance channel potential dies out. Due to this, the nuclear field of target nucleus does not remain strong enough to capture all the nucleons. Accordingly transfer of fractional momentum takes place leading to onset of ICF process. As a consequence of ICF,

(i) The reduced CN is formed with relatively lesser mass and charge in comparison to the total mass and charge of interacting species in CN reactions.

(ii) The reaction products have lesser recoil velocity as compared to that of complete fusion population.

The pictorial description of the process of incomplete fusion can be understood as follows:

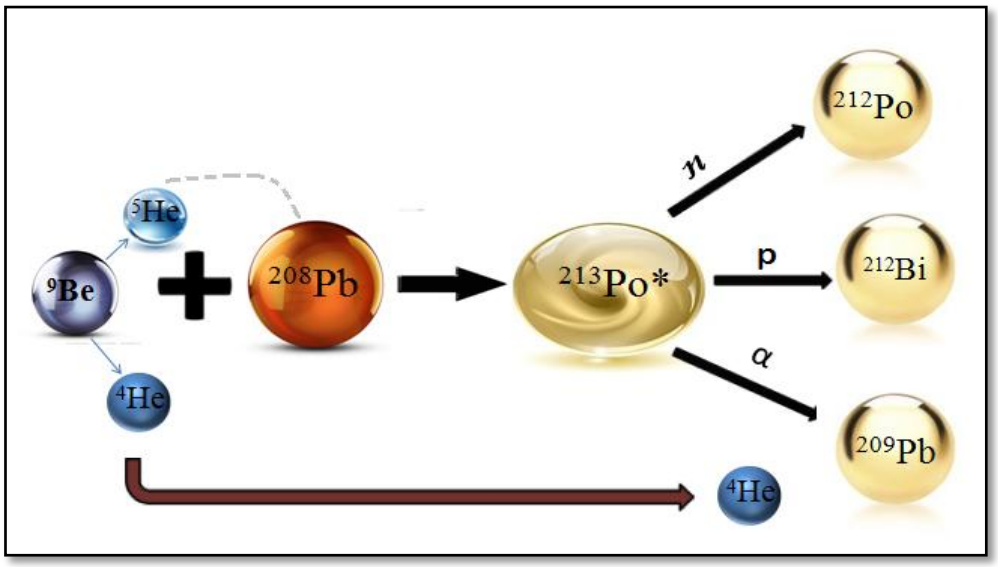

Fig 1.3: A part of projectile that passes without striking to target in process of incomplete fusion

The mass transfer, in case of ICF processes, occurs mainly from lighter to heavier partner, the feature being more prominent for asymmetric systems with respect to mass (at energies around 10 MeV per nucleon) as compared to symmetric ones. It is also named as breakup fusion, massive transfer, pre-compound emission or prompt emission of particles [5].

1.2.2 Decay of Compound Nucleus

In general, the decay mechanism of the compound nucleus is essentially treated using statistical processes where eventually one or a group of nucleons tend to occupy sufficient energy to escape from the compound nucleus barrier. Depending on the interaction of incident beam, the hot and the rotating compound nucleus is internally excited during collision, and decays by emitting radiation, charged particle or heavier nuclei as shown in the figure below:

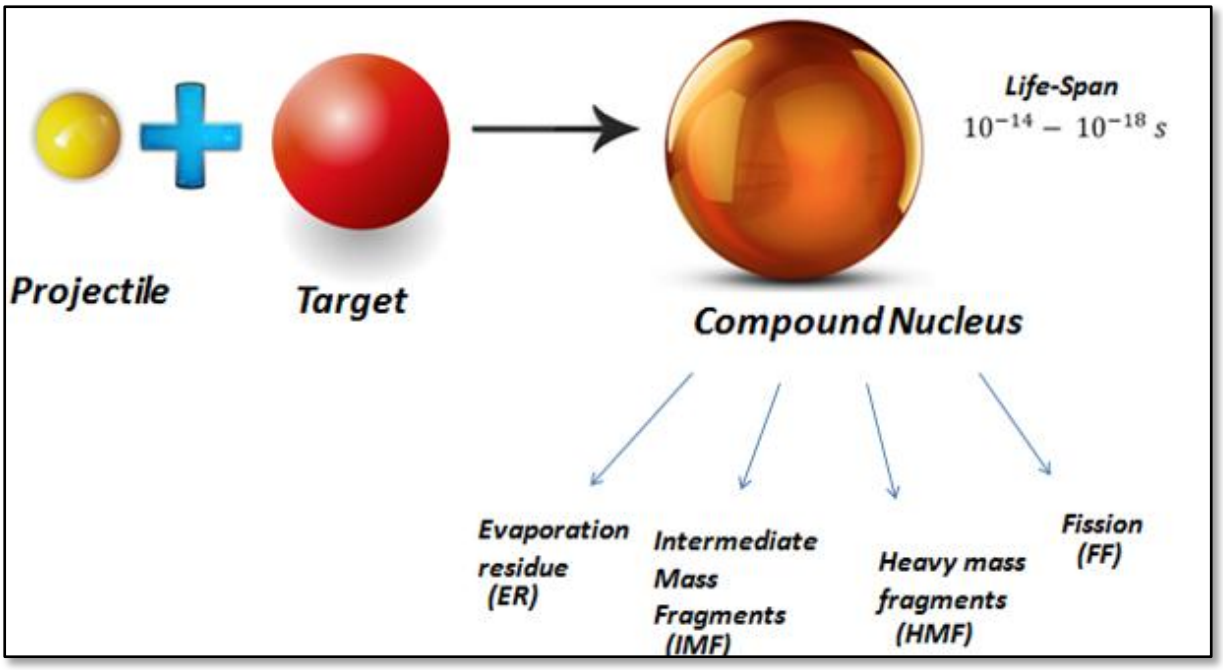

Fig 1.4: Decay of compound nucleus

According on the mass of compound nucleus formed, there exists a competition between light particle emission/evaporation residue (ER) and nuclear fission. For compound systems with lighter mass range A_{CN} ~ 40-80, the emission of light particles also known as evaporation residue (A_2= 1-4) is most dominant decay channel accompanied by intermediate mass fragments (IMFs) having quite a small contribution. The IMFs are the fragments falling in the range $5 \leq A_2 \leq 20$ [6]. However for the heavy mass nuclear systems, due to its instability against centrifugal repulsion, fission comes out to be the most probable decay mode which is discussed ahead. Besides this, heavy mass fragments (HMFs), the fragments possessing mass between IMFs and those of fission fragments are also observed in some of the heavy ion reactions.

There has been an emerging interest in the field of reaction dynamics of weakly bound nuclei in recent years. The internal structure of these nuclei departs from the conventional spherical structure and has small separation energy. The recent availability of radioactive beams marks the intriguing scrutiny of weakly bound nuclei. Such nuclei mostly break into charged fragments which in turn make the

breakup measurements with loosely bound nuclei experimentally advantageous as comparatively it is easier to detect fragments than neutrons [7].

1.2.2.1 Fission

The discovery of nuclear fission came into existence by the efforts of Otto Hahn and Fritz Strassmann, in 1939. Neutron discovery by Chadwick was perchance the most important key which opened the door to fission. The liquid drop model showed that there are two main factors controlling the energetics of fission mainly the surface energy of the drop along and Coulomb energy stored within the nucleus. This model concluded that the condition must hold true, for fission to occur that each and successive differential in distortion must lead to a system of lower potential energy than the initial spherical object. Nuclear fission is a complex process producing a wide range of nuclei and other radiations. It can be regarded as a process that involves a large scale rearrangement of the constituents of nucleus (nucleons) splitting into two fragments of comparable mass at final stage. The study of the fission dynamics at high excitation energy is anticipated to provide information about the magnitude and nature of nuclear dissipation by measuring the total fission cross sections [8].

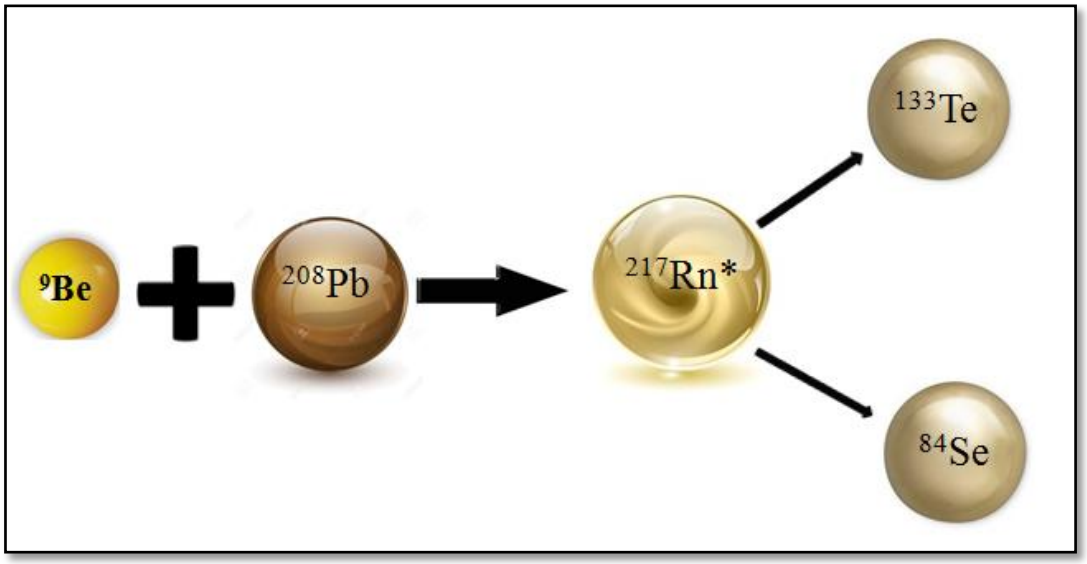

Fig1.5: Mechanism of fission for given reaction

The sum of masses of the fragments formed is less than the original mass of nucleus which we now call it as mass defect. In spite of the fact that fission phenomenon has

been uncovered several years back, it continues to remain a challenging zone even today, henceforth considerable efforts are needed to understand its peculiarities, by examining the collective participation of nucleons within the deformed shapes of nuclear entities [9]. For the compound nucleus with mass A≥200, that forms a range of heavy deformed targets, Coulomb repulsion increases more rapidly than nuclear binding energy leading to the symmetric or asymmetric fission products as a consequence. In case of the symmetric product, the mass distribution is centred on one mean value (≈A/2) while on the other hand asymmetric fission is represented by a double humped structure in the fission region. There are several cases where LP's or ER appears along with fission fragments and thus the comparative analysis of fission and ER provide important inputs for overall conceptualization of the dynamics of reaction under consideration.

1.2.3 Non Compound Nuclear Reactions

In addition to compound nucleus processes, depending on the several factors such as entrance channel, mass asymmetry and incident energy, a few processes having interaction time shorter than the lifetime of compound nucleus but long enough for exchanging mass energy, start competing are termed as non compound nuclear reactions. In these reactions, the projectile interaction with the target may reseparate prematurely before a fully equilibrated compound nucleus is formed. Probably the simplest quantitative distinction between CN and nCN mechanisms lies in their interaction times. As an anamoly to CN, the nCN mechanisms generally keep hold of the history of its formation. These processes also contribute in providing interesting information about nuclear structure and the reaction dynamics. Alike compound nucleus processes, various processes fall under the category of non compound nucleus process too e.g. quasi fission and deep inelastic collision which are discussed in subsequent sections.

1.2.3.1 Quasi fission

Among various nCN processes, the process of quasi-fission emerges out to be a dominant decay mode marked by the formation of composite systems that do not

reach the fully equilibrated compound nucleus state before it gets split in two fission-like fragments [10]. This may be attributed to the high fusion barrier in comparison to projectile energy due to which the composite system decays in a very short time (as compared to the formation of equilibrated CN) so as to acquire near mass symmetry.
The characteristics and the probability of quasi fission products are determined by the diffusive motion over a multi-dimensional potential energy surface (PES) [12]. Theoretically QF is predicted for the charge product Z_pZ_t> 1600 [13]. But recent studies on a number of compound systems formed via entrance channel having Z_pZ_t<1000 revealed the presence of quasi-fission across the barrier. The studies have depicted that the process of quasi fission may arise from physical origins like

- From vanishing of the fission barriers at high angular momentum.
- From trajectories of the system in the potential landscapes that lead to fast separations of the partners.
- Due to the disappearance in the potential of the compound nucleus minimum, thus making fusion impossible.

And it can lead to broader mass distributions or higher most probable kinetic energies for fission like fragments which further influence the CN formation and inhibit the formation of super heavy elements [13].

1.2.3.2 Deep Inelastic Collision (DIC)

The deep inelastic scattering process has imparted most of our understanding on mass rearrangements in heavy ion reactions (HIRs).When a heavy ion collide around the grazing impact parameters and the exit channel still essentially being binary, the collision is said to be deep inelastic collision(DIC). DIC lies between fusion-fission reaction that proceeds via central collision and peripheral collision involving only few nucleon degrees of freedom. The process of such collision is also termed as relaxed peak processes or strongly damped collisions. Damped or deep inelastic collisions are characterized by mass exchange as well as the damping of substantial kinetic energy while retaining the memory of entrance channel masses and charges partially [14]. Such processes appear at high bombarding energies. During brief encounter of the two

nuclei, the dissipation huge amount of kinetic energy of radial and orbital motion follows. During the course of decay, while dissociation of compound nuclei into fragments, the total kinetic energies of the fragments can be fairly below the Coulomb repulsion of products indicating a high degree of deformation of the fragments in the exit channel. These deep inelastic or damped collisions usually occur for heavy ion reaction at $E_{c.m.}$(centre of mass energies) less than 5MeV per nucleon above the Coulomb barrier [15]. DIC is not characterized by the full momentum transfer as the composite system in DIC does not get trapped in the pocket of nucleus potential. In DIC, the time of interaction for the composite system, bridges the gap between CN and QF process. It is observed often in reactions involving light mass nuclei, for partially damped waves close to the grazing angle and with product masses alike projectile and target mass.

1.3 Importance of the present work

In recent experiment [7], ^{9}Be was used as the common projectile to form two different compound nuclei. As it is weakly bound projectile, thus it may lead to incomplete fusion due to its loosely bound characteristic. So it would be of interest for us to study the complete fusion with this projectile, as the weakly bound nuclei deviate from the conventional spherical structure and have small separation energy. When such weakly bound nucleus tends to collide with target nucleus then its probability of break up gets enhanced. There is a notable interest in this field due to the contemporary run of radioactive beams of weakly bound nuclei [14]. Further, the reactions with weakly bound nuclei can serve to distinguish the complete fusion and incomplete fusion with the help of evaporation residues emitted in the two reactions. Such nuclei mostly break into charged fragments which in turn make the breakup measurements with loosely bound nuclei experimentally advantageous as comparatively it is easier to detect fragments than neutrons [15]. In nuclear fragmentation reaction light nuclei with exotic combinations of neutrons and protons are produced which extend to the very limits of nuclear stability, the neutron and proton drip lines. In such nuclei, some of the constituent protons or neutrons venture around the core of the nucleus, forming

a misty cloud termed as halo nuclei which can be envisaged to form a special case of weakly bound nuclei.

The study of reactions involving loosely bound nuclei has been of great interest in recent times. This is due to the fact that the binding energy of these nuclei is small in comparison other stable nuclei. The average binding energy of a stable nucleus is around 6-8 MeV but in case of halo nuclei, the binding energy is around 1 MeV. As a result reactions involving loosely bound nuclei have low breakup threshold. The presence of such nuclei may result into various features such as the suppression or enhancement of the nuclear cross sections for energy region above the Coulomb barrier. Due to extended structure in comparison to ordinary nuclei, relatively easier penetration through the potential barrier is observed, causing enhancement in the cross-sections. On the other hand, such nuclei being loosely bound may also witness an increase in probability of breakup of original projectile and lead to the fusion of residual nucleus (obtained after break-up) with the target nucleus giving rise to suppression in cross-sections and hence the onset of incomplete fusion[16].

In this work, an extensive analysis is carried out in reference to decay profile of ^{9}Be +^{208}Pb and ^{9}Be +^{209}Bi reactions performed over a wide range of incident energies. The probability of light particle emission and fission is exercised and related fragmentation behaviour is examined in order to have better understanding of dynamical aspects of these reactions. In addition to this, by keeping in mind about loosely bound characteristics of ^{9}Be, the study of incomplete fusion process has been taken into consideration. The calculations are carried out using dynamical cluster decay model (DCM), the brief details of which are described in Chapter 2. Finally the results obtained and conclusions drawn are described in Chapter 3.

References

[1] S. N. Ghoshal Phys. Rev. **80**, 6 (1950).

[2] M. Dasgupta, D. J. Hinde Phys. Rev. Lett. **82**, 7 (1999).

[3] M. Singh, Sukhvinder et al. Nucl. Phys. A **897,** 179–197 (2013).

[4] L.F. Canto et al. Nucl. Phys. A **821,** 51-71 (2009).

[5] L. F. Canto, R. Donangelo, and Lia M. de Matos Phys. Rev. C **58**, 2 (1998).

[6] B. Singh, M. K. Sharma Phys. Rev. C **77**, 054613 (2008).

[7] M. Dasgupta Phys. Rev. C **81**, 024608 (2010).

[8] J. Benlliure a, P. Armbruster et al. Nucl. Phys. A **700,** 469–491 (2002).

[9] N. Bohr, Phys. Rev. **56**, 1 (1939).

[10] D. J. Hinde, M. Dasgupta et al. Journal of Physics: Conference Series **420,** 012115 (2013).

[11] D.J. Hinde, R. du Rietz EPJ Web of Conferences **66,** 03037 (2014).

[12] E. Prasad, K. M. Varier et al. Phys. Rev. C **81**, 054608 (2010).

[13] M. Morjean, D. Jacquet et al. Journal of Physics: Conference Series **282,** 012009 (2011).

[14] T.Mikhailova, M.Colonna et al. Rom. journ. Phys **52,** (2007).

[15] T. Ishii, M. Itohb, et al. Nuclear Instruments and Methods in Physics Research A **395**, 210 (1997).

[16] E. Prasad, K. M. Varier et al. Phys. Rev. C **84**, 064606 (2011).

Chapter II

Methodology

Chapter-II

The Dynamical Cluster Decay Model (DCM)

2.1 Introduction

The Dynamical Cluster-Decay Model (DCM) [1-7] is an transformation of the preformed cluster model (PCM) of for ground- state decays, which itself is planted on the well known Quantum Mechanical Fragmentation Theory, the QMFT [8-9], given for fission as well as heavy ion reactions.

This model is a non statistical characterization of the various decay processes having contribution from compound nucleus (CN) as well as non compound nucleus (nCN) mechanisms, each calculated as a dynamical fragmentation process. The cross-sections constitute of either evaporation residues and fission fragments, including intermediate as well as heavy mass fragments, each calculated in one set of calculation in reference to mass asymmetry parameter η= (A_1-A_2) / (A_1+A_2). The cross sections are estimated in terms of their pre-formation probability P_0 and barrier penetration probability P.

In other words, we explicate the decay cross-sections in partial wave analysis terms as:

$$\sigma = \frac{\pi}{k^2} \sum_{l=0}^{l_{max}} (2l+1)\, P_0 P \qquad (1)$$

with k given by k= $\sqrt{\frac{2\mu E_{cm}}{\hbar^2}}$

The reduced mass:-

$$\mu = \left[\frac{A_1 A_2}{(A_1 + A_2)}\right] m = \frac{1}{4} Am(1 - \eta^2)$$

Where m is the nucleon mass and ℓ_{max} is the maximum angular momentum affix for the vanishing fusion barrier of the entrance channel η_i or the cross section of light particle emission $\sigma_{LP} \rightarrow 0$.

In Eq. (1), P_0 is preformation probability and P, penetrability refering to η (asymmetry) motion and R motion respectively. Apparently, the two motions are seized as decoupled, as discussed in earlier works [9]

We solve the stationary Schrödinger equation for η-motion, in the form of η, at a fixed relative separation R, and that equation is given as follow:-

$$\left\{-\frac{\hbar^2}{2\sqrt{B_{\eta\eta}}}\frac{\partial}{\partial\eta}\frac{1}{\sqrt{B_{\eta\eta}}}\frac{\partial}{\partial\eta}+V_R(\eta,T)\right\}\psi^{\nu}(\eta)=E^{\nu}\psi^{\nu}(\eta) \qquad (2)$$

With ν = 0, 1, 2, 3….where (ν = 0) refers to ground state and other greater values refer to the excited state solutions.

$B_{\eta\eta}$ (η) is smooth classical hydro dynamical masses [10] and represents the kinetic energy part. The solutions of Eq. (2) give the pre-formation probability,

$$P_0 = \sqrt{B_{\eta\eta}} \mid \Psi[\eta(A_i)] \mid^2 (\tfrac{2}{A}) \qquad (3)$$

Where (i =1 or 2), and $\psi(\eta)$ is $\psi^{\nu=0}(\eta)$ if the ground-state solution is taken. The deformation and orientation dependent fragmentation potential is given as:

$$V_R(\eta,T)=\sum_{i=1}^{2}[V_{LDM}(A_i,Z_i,T)]+\sum_{i=1}^{2}[\delta U_i]\exp(-T^2/T_0^2)+V_c(R,Z_i,\beta_{\lambda i},\theta_i,T) \qquad (4)$$
$$+V_P(R,A_i,\beta_{\lambda i},\theta_i,T)+V_\ell(R,A_i,\beta_{\lambda i},\theta_i,T)$$

Where, the T-dependent liquid drop energy $V_{LDM}(T)$ is that of [11], with (Seeger's) constants at $T=0$ refitted to give binding energies of [12], defined as $B=V_{LDM}(T=0)+\delta U$, the shell corrections are calculated in the "empirical method'' of Myers and Swiatecki [13].

The V_P is the nuclear proximity potential, considered to be temperature dependent here and is given by:

$$V_P(s_o(T))=4\pi\bar{R}(T)\gamma b(T)\phi(s_o,(T)) \qquad (5)$$

where $\bar{R}(T)$ and $\phi(s_o,T)$ are, respectively, the inverse of the root mean square radius of the Gaussian curvature and the universal function, which is independent of the geometry of the system, given by:

$$\phi(s_o,T)=\begin{cases}-\frac{1}{2}(s_o(T)-2.54)^2-0.0852(s_o(T)-2.54)^3\\-3.437\exp(-s_o(T)/0.75)\end{cases} \quad (6)$$

For $s_o(T)\le 1.2511$ and $s_o(T)\ge 1.2511$ respectively, and γ is the specific nuclear surface tension and is given by:

$$\gamma=0.9517\left[1-1.7826\left(\frac{N-Z}{A}\right)^2\right]\mathrm{MeV\,fm^{-2}} \quad (7)$$

The same temperature dependence of R(T) is also used for Coulomb potential $[V_C(T)=[\frac{Z_1Z_2e^2}{\mathrm{R(T)}}]$ where Z_i are fixed by minimizing the potential $V_R=\eta T$ in the coordinates of charge asymmetry $\eta_z=(Z_1-Z_2)/(Z_1+Z_2)$.The shell corrections δU in the Eq.(4) start vanishing beyond $T_0=1.5$ Mev.

Also, for the angular momentum effects

$$V_\ell(T)=\frac{\hbar^2\ell(\ell+1)}{2I(T)} \quad (8)$$

The moment of inertia in Eq.(8) is given by

$$\mathrm{I(T)}=I_{NS}(\mathrm{T})=\mu R_a^2 \quad (9)$$

The separation distance R, in this case, is presumed to be afar the range of nuclear proximity forces, which is about 2 fm. However, when it is within the range of nuclear proximity (< 2 fm), the moment of inertia lies in the complete sticking limit as:

$$\mathrm{I(T)}=I_S(\mathrm{T})=\mu R_a^2+\frac{2}{5}A_1mR_1^2+\frac{2}{5}A_2mR_2^2 \quad (10)$$

The compound nucleus temperature T (in MeV) related as

$$E_{CN}^*=\left(\frac{A}{9}\right)T^2-T \quad (11)$$

The preformation factor P_0, at temperature T in Eq. (3) is calculated at R_a which is given by $R_a=R_t(\eta)+\Delta R$, including temperature effects in $\Psi(\eta)$ through a Boltzmann-like function $|\Psi|^2=\sum_{\nu=0}^{\infty}|\Psi^\nu|^2\exp(-\frac{E^\nu}{T})$

The penetrability P is calculated as the WKB tunneling probability, solved analytically, as

$$P=\exp[-\frac{2}{\hbar}\int_{R_a}^{R_b}\{2\mu[V(R)-Q_{eff}]\}^{1/2}dR] \quad (12)$$

For hot compound nucleus decay, the first turning point R_a is defined as $R_a = R_t(\eta) + \Delta R = R_i(\alpha_i, T) + \Delta R(T)$

ΔR is the relative separation distance or the neck formed after the fusion of incoming channel between two fragments or clusters A_i. The radius vector is given by:

$$R_i(\alpha_i, T) = R_{0i}(T)[1 + \sum_{\lambda i} Y_\lambda^{(0)}(\alpha_i)]$$

This value of R (besides R_0, the compound nucleus radius) incorporates to a sufficed extent the upshot of both deformations β_i of two fragments as well as neck formation between them. The temperature dependence in radii R_{0i}, in the definition of R_a, is given as [14].

$$R_{0i} = [1.28A_i^{1/3} - 0.76+0.8A_i^{-1/3}](1 + 0.0007T^2) \quad (13)$$

With the surface width

$$b(T)=0.99(1+0.009T^2) \quad (14)$$

In context of the two-centre shell model, used to govern shell effects δU, ΔR is shown to incorporate the effects of neck formation [15, 16], thus referred as the neck length parameter. The potential corresponding to R_a, V_R behave like an effective, positive Q value. For hot compound nucleus decay at temperature T, Q_{eff} of two fragments in the exit channel is noticed in the ground states at (T = 0). Thus Q_{eff}, in terms of the respective binding energies, is defined as:

$$Q_{eff}(T) = B(T) - [B_1(T=0) + B_2(T=0)] = \text{TKE (T)} = V(R_a) \quad (15)$$

For the penetrability P,

$$V(R_a) = V(R_t + \Delta R) = V(R_b) = Q_{eff} = \text{TKE(T)} \quad (16)$$

With R_b, as the second turning point.

To calculate the energy of ICF component, one may do appropriate correction in the incident energy as stated in [17]

On the footing of degree of linear momentum transfer (LMT) from the projectile to target, the untwining of CF and ICF events can be done. The entire nucleonic degrees

of freedom of projectile as well as target nucleus combine to form an equilibrated compound nucleus in the case of CF and predetermine the physical properties such as mass charge, recoil velocity etc. Nonetheless the ICF events contrive from LMT followed by loosely bound projectile breakup.

After having some idea about the methodology adopted to estimate ER and fission of heavy ion induced reactions some calculations are performed by striking a loosely bound projectile ^{9}Be on stable targets ^{208}Pb and ^{209}Bi. The results are summarized in the next chapter.

References

[1] R. K. Gupta, M. Balasubramaniam, R. Kumar, D. Singh, C. Beck and W. Greiner, Phys. Rev. C **71**, 014601 (2005).

[2] R. K. Gupta, M. Balasubramaniam, R. Kumar, D. Singh, S. K. Arun and W. Greiner, J. Phys. G: Nucl. Part. Phys. **32**, 345 (2006).

[3] G. Kaur, D. Jain, R. Kumar and M. K. Sharma, Nucl. Phys A **916,** 260 (2013).

[4] G. Sawhney, G. Kaur, M. K. Sharma and R. K. Gupta, Phys. Rev. C **88,** 034603 (2013).

[5] M. Kaur and M. K. Sharma, Eur. Phys. J. A 5**0,** 61 (2014).

[6] K. Sandhu. G. Kaur and M. K. Sharma, Nucl. Phys. A **21,** 114 (2014).

[7] S. K. Arun, R. Kumar and R. K. Gupta, Jour. Phys. G: **36**, 085105 (2009).

[8] J. Maruhn and W. Greiner, Phys. Rev. Lett. **32**, 548 (1974).

[9] R. K. Gupta, W. Scheid, and W. Greiner, Phys. Rev. Lett. **35**, 353 (1975).

[10] H. Kroger and W. Scheid, J. Phys. G Nucl. Phys. **6**, L85 (1980).

[11] N. J. Davidson, S. S. Hsiao, J. Markram, H. G. Miller, and Y. Tsang, Nucl. Phys. A **570**, 61C (1994).

[12] G. Audi and A. H. Wapstra, Nucl. Phys. A **595**, 4 (1995).

[13] W. Myers and W. J. Swiatecki, Nucl. Phys. A **81**, 1 (1966).

[14] G. Royer and J. Migner, J. Phy. G **18**, 1781 (1992), and earlier references therein.

[15] S. Kumar and R. K. Gupta, Phys. Rev. C **55**, 218 (1997).

[16] R. K. Gupta, S. Kumar, and W. Scheid, Int. J. Mod. Phys. E **6**, 259 (1997).

[17] G. Kaur and M. K. Sharma, Nucl. Phys. A **884**, 36, (2012).

Chapter III

Results and Discussions

Chapter III

3.1 Results and Discussion

Reactions having projectiles of relatively lesser binding energy i.e. the nuclei possessing weakly bound characteristic have been spaciously studied in the last few years. Aforesaid inquisition has major importance for the study of light systems in the context of astrophysics, where radioactive nuclei possessing low energy can produce multiple reactions by interacting strongly. There has been a growing interest on how the breakup of radioactive weakly bound and stable nuclei can affect on the fusion cross-sections, at energies in vicinity of barrier. Intrinsically, the nuclei acquiring less mass may positioned around or far from the stability line can show exhibit exotic characteristics as well as structures, halo nuclei being one of them comprising a special case of weakly bound nuclei. Consequently, researchers may explore new conceptions as well as various domains of reaction mechanism to study the exotic characteristic and structure with the help of reactions involving such kind of nuclei, which will be totally different from the mechanisms used for stable nuclei. Hence, in reference to experiment [1], an attempt has been made to address the reaction dynamics of weakly bound nucleus (^{9}Be) induced reactions, by reacting it with two stable targets, one being the doubly magic $^{208}_{82}Pb$ and other being $^{209}_{83}Bi$.

In the recent experiment [1], the reactions in which ^{9}Be incident on ^{208}Pb and ^{209}Bi have been performed at above barrier energies to investigate distinctions in their reported complete fusion cross-section. The current analysis show that the above barrier complete fusion cross-section of ^{217}Rn* and ^{218}Fr* are formed by using same projectile (^{9}Be) are very similar. Contrarily fission cross sections are much larger for heavier target ^{209}Bi.

In view of above, it is important to carry out a comparative analysis of ER and fission cross-sections on above mentioned target-projectile combination. It is substantial to mention here that $\boldsymbol{\sigma}_{CF} = \boldsymbol{\sigma}_{ER} + \boldsymbol{\sigma}_{Fission.}$ Therefore $\boldsymbol{\sigma}_{ER}$ is estimated from available data of [1], and consequently the fission and ER data is addressed by using dynamical cluster decay model (DCM) based analysis. Here an attempt has been made to fit the

evaporation residue and fission cross-sections using the only parameter of DCM [2-8] i.e. neck length parameter for the following reactions.

$$^{9}Be + {}^{208}Pb \rightarrow {}^{217}Rn^{*} \rightarrow A_1 + A_2$$

$$^{9}Be + {}^{209}Bi \rightarrow {}^{218}Fr^{*} \rightarrow A_1 + A_2$$

The calculations have been carried out by using β_2-deformed choice of fragmentation within optimum orientation approach. Interestingly, at all energies, the evaporation residues ($A_2 \leq 4$) form the most contributing decay process.

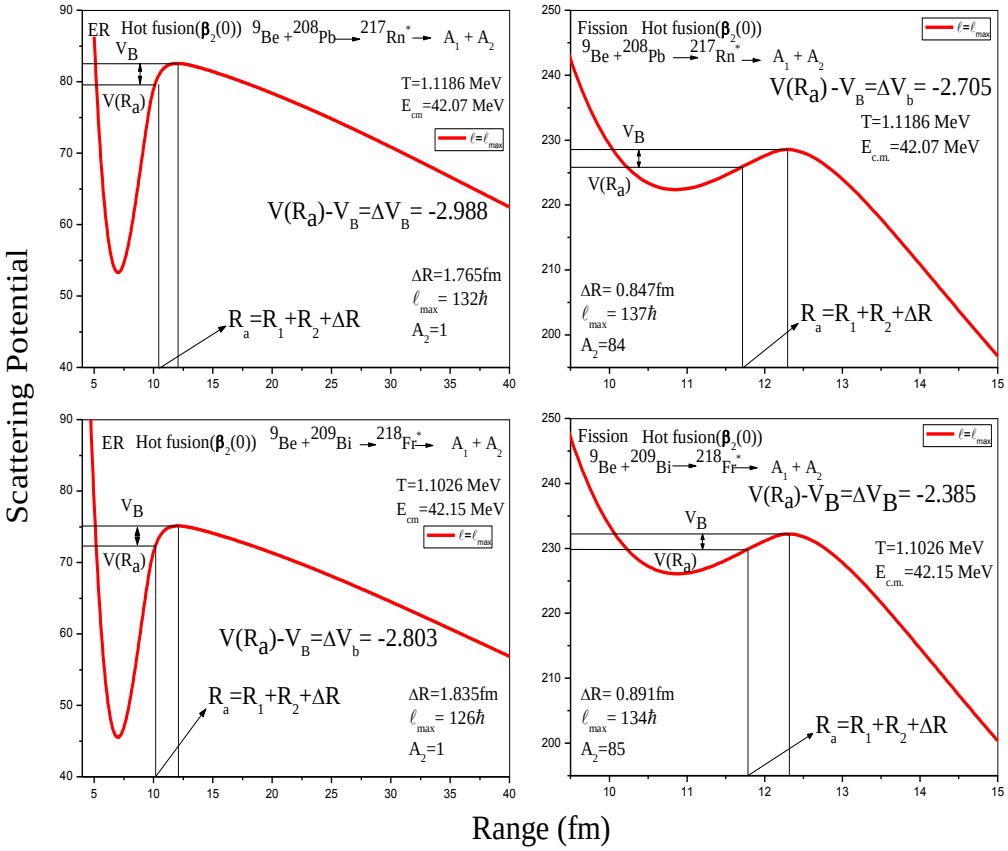

Figure 3.1. *Scattering Plot for $^{217}Rn^{*}$ and $^{218}Fr^{*}$ for fission and Evaporation Residue at lowest energies for maximum angular momentum.*

Further to observe the decay mechanism of $^{217}Rn^{*}$ and $^{218}Fr^{*}$, the neck length parameter ΔR (T) allows us to equivalently determine the barrier lowering parameter ΔV_B which directly relates

$$\Delta V_B = V(R_a, \ell) - V_B(\ell).$$

and can be seen in fig 3.1, which demonstrate the variation of scattering potential as a function of relative distance R, by which we are able to access the energy transfer process at extreme ℓ value. It is clearly evident from the figure that barrier height is more for $^{217}Rn^{*}$ as compared to $^{218}Fr^{*}$ for both choice of decays.

The point to notify here is that barrier height and angular momentum increase as we move from evaporation residue to fission for both compound nuclei. The barrier penetration point R_a is much higher for fission decay as compared to that of evaporation path. Also the barrier lowering parameter ΔV_B is defined as $V(R_a) - V_B$, is higher in magnitude for ER as compare to fission. The subsequent details of barrier modification and its relevance in context of fragmentation calculations are described later in fig. 3.4 and 3.5. Further to study the decay characteristics of $^{217}Rn^{*}$ and $^{218}Fr^{*}$ nuclei, we have investigated the behaviour of various properties such as fragmentation potential, preformation factor, neck length, and barrier modification etc.

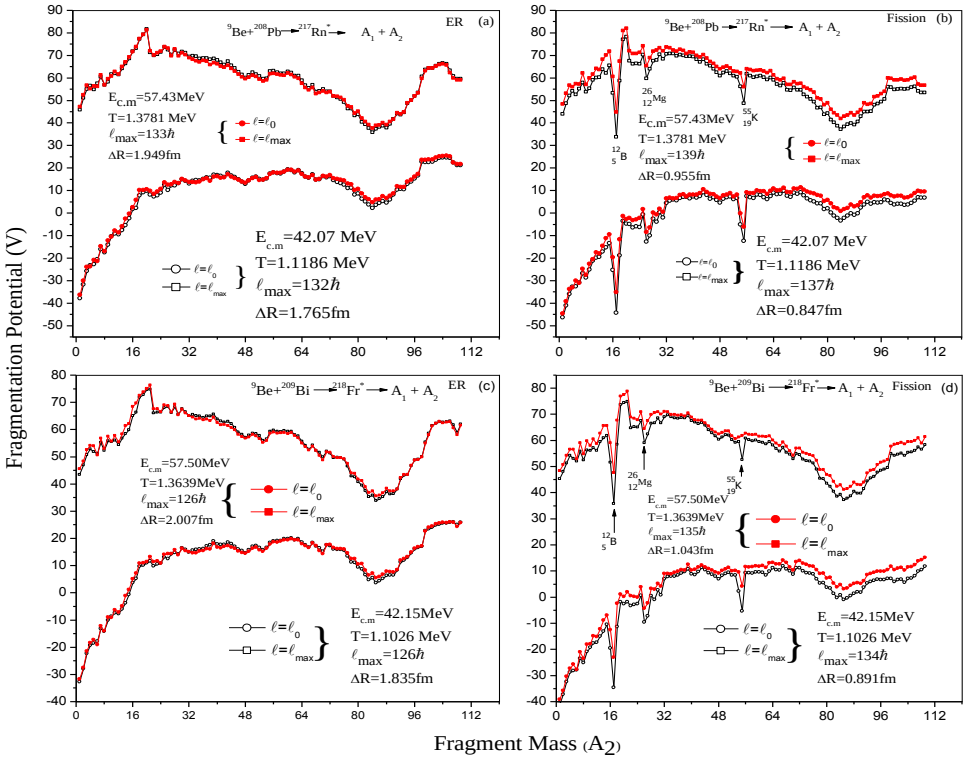

Fig 3.2 *Fragmentation potential as a function of fragment mass (A_2) for β_2-deformed choice of fragmentation at extreme energies for (a),(b) $^{217}Rn^{*}$ and (c), (d) $^{218}Fr^{*}$*

It may be noted that in DCM based calculations, the minima in fragmentation potential leads to maxima in preformation probability which eventually results into higher magnitude of cross-sections for that decaying fragment. Interestingly, excluding the minor change in magnitude, there is no momentous change in the potential energy surface (PES) at two extreme energies plotted in figure 3.2. However, the neck length parameter ΔR, increases with increment of energy for both choice of decays i.e. ER and fission. Figure 3.2 (a) and (b) describe the fragmentation behaviour of $^{217}Rn^{*}$ formed in $^{9}Be + ^{208}Pb$ reaction, for ER and fission dynamics respectively. It is evident from figure 3.2 (a) and (b) that the fragmentation path is almost identical at two extreme energies, for both ER and fission decay. Also, independent of decay choice, the asymmetric pattern of fragmentation is observed. Although some abrupt dips may be observed in IMF/HMF region while going from ER to fission analysis, but they don't contribute significantly towards the overall fusion cross sections and ergo can be ignored. Figure 3.2 (c) and (d) depicts the same results, but for the decay of $^{218}Fr^{*}$ formed in $^{9}Be + ^{209}Bi$ reaction.

It may also be noted that as we move from ER to fission decay, ℓ_{max} value is found to increase, though neck length parameter is less in case of fission as expected on the basis of our earlier analysis [9]. As the structural report of compound nucleus penetrate in the DCM via preformation probability P_0, thus the variation of preformation probability as a function of fragment mass is plotted in fig 3.3 for $^{217}Rn^{*}$ and $^{218}Fr^{*}$ nuclei.

Figure 3.3 demonstrate the preformation probability (P_0) as a function of fragment mass (A_i) for $\ell=0\hbar$ and $\ell=\ell_{max}$ at extreme energies using β_2-deformed choice of fragmentation for evaporation residue as well as fission channels. It can be seen from fig 3.3 (a) and (b) that preformation profile exhibit a clear asymmetric distribution for ER as well as fission channel for $^{217}Rn^{*}$ system. The fragments in the range A_2 = 80-90, seem to contribute towards the fission pattern. It may be noted that the preformation probability of the asymmetric fragments is comparably higher in case of fission as compared to that of evaporation residue. Similar calculations has been performed for $^{218}Fr^{*}$ system as shown in fig 3.3 (c) and (d) at extreme energies. As

evident from fig. 3.3, $^{217}Rn^{*}$ and $^{218}Fr^{*}$ nuclei formed in ^{9}Be induced reactions, exhibit almost similar preformation profile, despite the fact that fission cross sections are much higher for the consideration of heavier target shown in table 3.1 and 3.2.

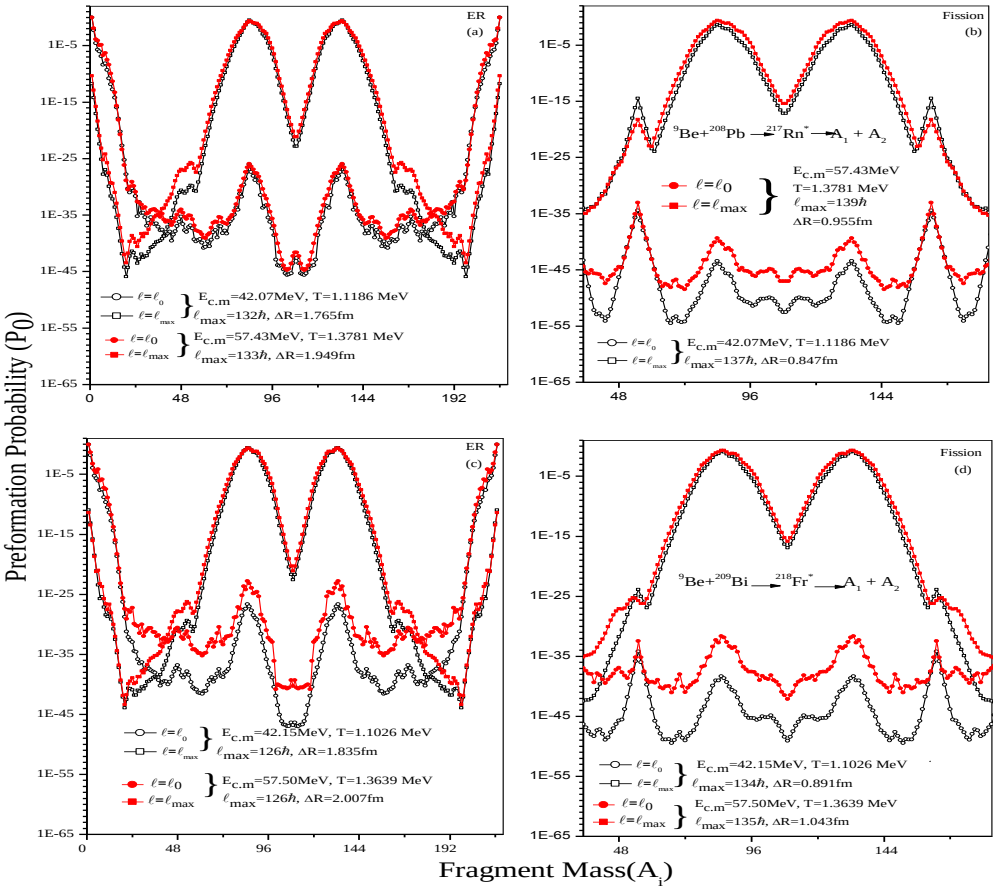

Fig 3.3 *Preformation Probability as a function of fragment mass (A_i) for β_2-deformed choice of fragmentation at extreme energies for (a),(b) $^{217}Rn^{*}$ and (c), (d) $^{218}Fr^{*}$*

Another significant quantity is the variation of barrier modification parameter i.e. ΔV_B. This property of barrier lowering in the vicinity of barrier energies is of even great pertinency and is an inbuilt property of DCM, that is included via neck length parameter ΔR used to fit the respective cross sections of $^{217}Rn^{*}$ and $^{218}Fr^{*}$ [1]. It has been calculated at different ℓ-values up to ℓ_{max} and to study its variation with angular momentum, we have plotted ΔV_B as a function of angular momentum shown in fig.

3.4 (a) and (b) for $^{217}Rn^{*}$, for ER and fission channel respectively. It is essential to address here that graph has been plotted considering to the most probable fission fragment and 1n channel for evaporation residue.

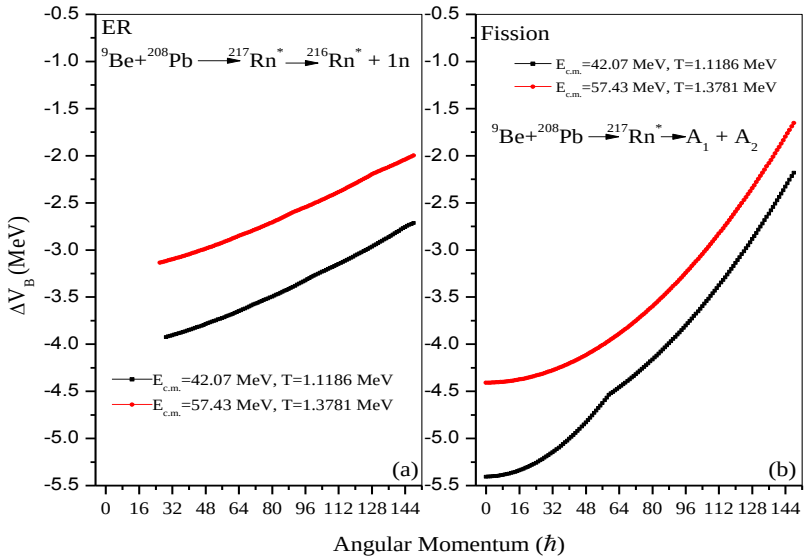

Fig 3.4. *Variation of barrier lowering parameter ΔV_B with angular momentum $\ell(\hbar)$ for $^{217}Rn^{*}$ nucleus at extreme energies below the Coulomb barrier for (a) ER and (b) fission.*

Also it is essential to know that the ΔV_B is negative and non zero for both decays. One can clearly see from fig. 3.4 that, there is rise in magnitude of ΔV_B with decrease in magnitude of angular momentum, and perceived to have minimum value at higher angular momentum. This observation indicates that ΔV_B is more important at lower ℓ-values for both decays i.e. ER and fission. In other words one may presume that larger magnitude of ΔV_B at lower incident energies (particularly below coulomb barrier) may play a significant role to address the fusion hindrance data, wherever applicable.

Furthermore, the variation of ΔV_B is plotted as a function of $E_{c.m.,}$ at $\ell=\ell_{max}$ for ER as well as for fission channels for the decay of $^{217}Rn^{*}$ as shown in fig. 3.5, One may observe that, ΔV_B starts decreasing with increase in incident energy of the system. The decrement as a function of centre of mass energy ($E_{c.m.}$) is almost linear for fission whereas, the same get saturated at larger incident energies in case of evaporation residue (ER). The same results of ΔV_B with ℓ and $E_{c.m.}$ are observed for $^{218}Fr^{*}$ (not shown here).

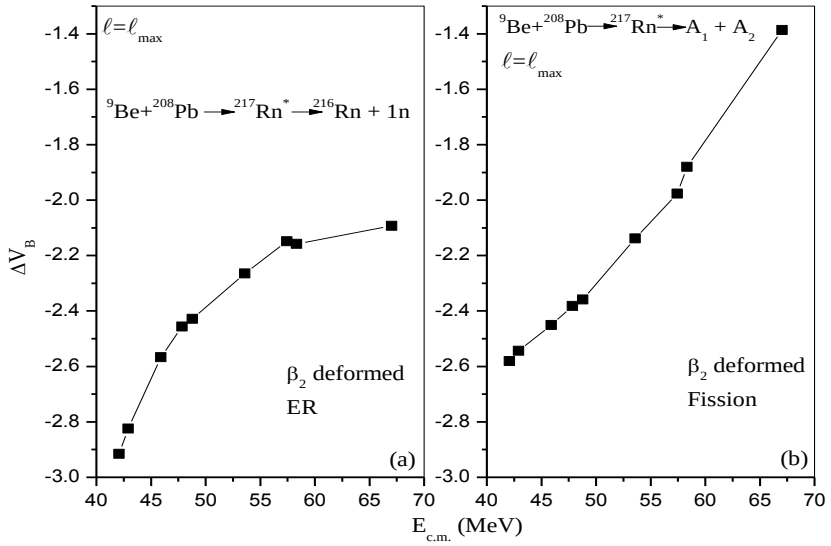

Fig3.5 *Variation of barrier lowering parameter ΔV_B with Centre of mass energy, $E_{c.m.}$ (MeV) for $^{217}Rn^*$ at $\ell=\ell_{max}$ for most probable decay fragment (a) ER (b) Fission*

As barrier modification parameter, ΔV_B has explicit dependence on the corresponding values of neck length parameter (ΔR), so it would be intriguing to see the revulsion of neck length parameter with $E_{c.m.}$, plotted in fig. 3.6 for both decay choices ER and fission.

Fig. 3.6 clearly shows that independent of decay path, the neck length parameter varies linearly with centre of mass energy ($E_{c.m.}$) and found to increase with increase in energy. Also in given experiment with same projectile ^{9}Be with different isotopic targets (^{208}Pb and ^{209}Bi) forming two different compound nuclei $^{217}Rn^*$ and $^{218}Fr^*$, the data for $^{217}Rn^*$ has been given upto $E_{c.m.}$ = 67.03 MeV although for $^{218}Fr^*$, it is only given upto $E_{c.m.}$ = 57.5 MeV. As the trend of variation is almost similar for both the nuclei, so the neck length parameter (ΔR) of $^{218}Fr^*$ is extrapolated to predict it upto $E_{c.m.}$ = 67.03 MeV shown in fig. 3.6 where open symbols represent the extrapolated values of neck length parameter (ΔR). Also, it can be distinctly seen from fig. 3.6 that ΔR is much smaller for fission as compare to ER, which seem to suggest that ER occurs at an early stage of nuclear dynamics and fission process takes relatively longer time.

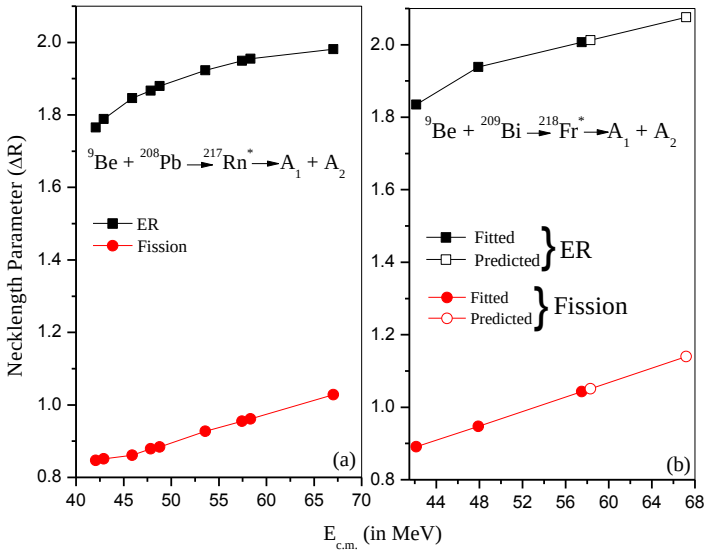

Fig. 3.6. *Variation of neck length parameter ΔR for fission and ER decay channel as a function of centre of mass energy, $E_{c.m.}$(Mev) for (a) $^{217}Rn^{*}$ (b) $^{218}Fr^{*}$*

All calculations have been accomplished using β_2-deformed choice of fragmentation, i.e. deformation effects up to quadrupole are included throughout the analysis, as shown in Table 3.1 and Table 3.2 for $^{217}Rn^{*}$ and $^{218}Fr^{*}$ respectively, which shows the variation of cross section as a function of centre of mass energy ($E_{c.m.}$).

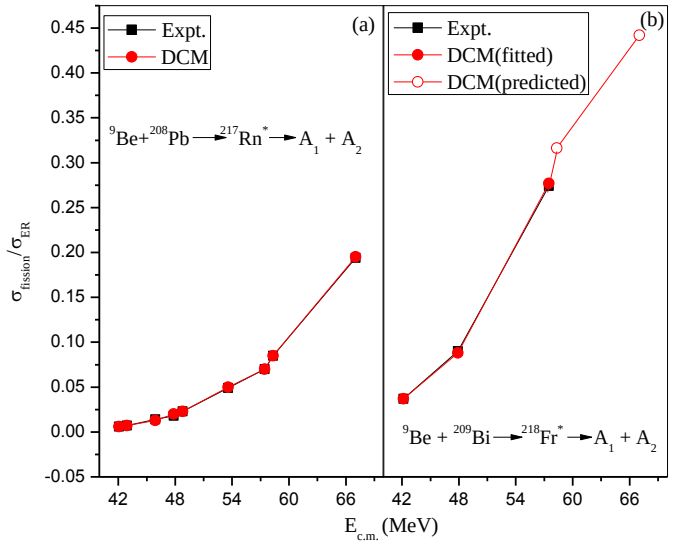

Fig 3.7. *Variation of ratio of fission to the evaporation residue cross-section as a function of centre of mass energy for (a) $^{217}Rn^{*}$, (b) $^{218}Fr^{*}$*

The DCM based results are in harmony with the experimental data for fission as well as for ER channel. From the table one can see that fission contribution is very small as compare to the evaporation, as also evident from fig. 3.7 which show the ratio of fission cross section to the evaporation residue cross section ($\boldsymbol{\sigma}_{\text{fission}}/\ \boldsymbol{\sigma}_{\text{ER}}$) for both compound nuclei $^{217}Rn^{*}$ and $^{218}Fr^{*}$.

As for $^{218}Fr^{*}$, the neck length parameter (ΔR) has been extrapolated for energies higher than $E_{c.m.}$ = 57.5 MeV. So the cross sections for both decay channels have been found at extrapolated ΔR at respective energies shown in table 3.2 and the ratio ($\boldsymbol{\sigma}_{\text{fission}}/\ \boldsymbol{\sigma}_{\text{ER}}$) of cross sections calculated by using these predicted ΔR at respective energies also shown (open symbols) in fig. 3.7 (b) along with fitted cross sections and the experimental data.

Table 3.1: *The ER and Fission cross-sections calculated using DCM for the $^{217}Rn^{*}$ nucleus formed in the ^{9}Be + ^{208}Pb reaction with the inclusion of quadrupole deformation, at all $E_{c.m.}$ values compared with the experimental data.*

$E_{c.m.}$ (MeV)	Temp. (MeV)	ℓ_{max} (ħ)		ΔR (fm)		σ_{DCM} (mb)		$\sigma_{exp.}$ (mb)	
		ER	Fission	ER	Fission	ER	Fission	ER	Fission
42.07	1.1186	132	137	1.765	0.847	227	1.402	227.62±6	1.38±0.03
42.92	1.1346	130	138	1.789	0.847	280	2.08	279.98±11	2.02±0.05
45.89	1.1886	130	139	1.846	0.861	438	6.00	437.85±11	6.15±0.06
47.84	1.2227	132	139	1.867	0.879	509	10.18	519.3±11	9.70±0.5
48.80	1.2391	130	139	1.880	0.884	543	12.84	544.2±12	12.8±0.09
53.58	1.3180	130	139	1.923	0.927	696	35	697.2±14	34.8±0.2
57.43	1.3781	133	139	1.949	0.955	786	55.6	789.52±10	55.48±.15
58.33	1.3918	130	141	1.955	0.961	805	69.2	808.9±17	69.1±0.3
67.03	1.5176	130	142	1.981	1.028	855	167	855.4±60	166.6±0.6

Table 3.2: *The ER and Fission cross-sections calculated using DCM for the $^{218}Fr^{*}$ nucleus formed in the ^{9}Be + ^{209}Bi reaction with the inclusion of quadrupole deformation, at all $E_{c.m.}$ values compared with the experimental data.*

$E_{c.m.}$(MeV)		Temp. (MeV)	ℓ_{max} (ħ)		ΔR(fm)		σ_{DCM}(mb)		σ_{exp}(mb)	
			ER	Fission	ER	Fission	ER	Fission	ER	Fission
Fitted	42.15	1.1026	126	134	1.835	0.891	227	8.48	227.42±7	8.53±0.09
	47.91	1.2075	126	134	1.939	0.947	504	44.8	504.29±12	45.71±0.23
	57.50	1.3639	126	135	2.007	1.043	685	190.0	696±14	190.4±0.6
Predicted	58.33	1.3766	127	136	2.009	1.048	685	216	-	-
	67.03	1.5032	127	136	2.071	1.138	892	394.18	-	-

The experiment performed to analyze the decay cross section of $^{217}Rn^{*}$ and $^{218}Fr^{*}$ [1] show that ^{9}Be can break in to ^{4}He and ^{5}He, which may further lead to incomplete fusion process. So an attempt has been made to investigate the incomplete fusion (ICF) in reference to the available experimental data [10].

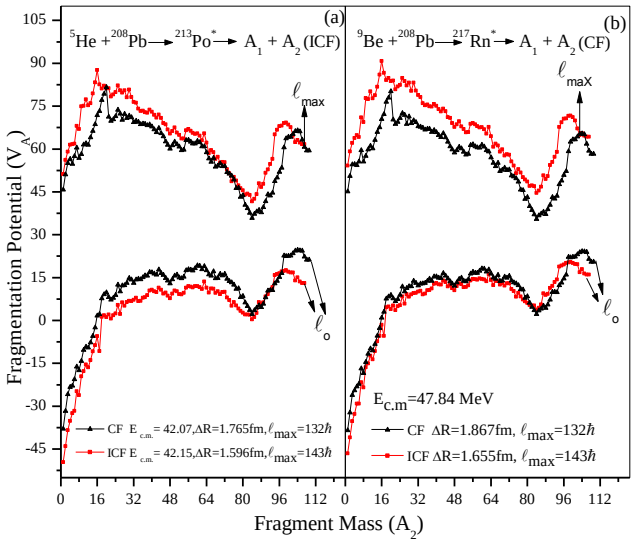

Fig 3.8 *Comparison of CF and ICF based Fragmentation potential as a function of fragment mass (A_2) for deformed fragmentation at (a) $E_{c.m.} \cong$ 42MeV and (b) $E_{c.m.}$= 47.84 MeV*

Based on the data [10], the contribution of ICF due to the breakup of ^{9}Be is studied by considering ^{5}He as active channel. The calculations have been done for $^{5}He + ^{208}Pb \rightarrow ^{213}Po^{*} \rightarrow A_1 + A_2$, with evaporation residue as the only decay channel at two energies ($E_{c.m.} \cong 42$ MeV and 47.84 MeV) for β_2-deformed. The fitted cross sections are consistent with experimental data, which shows that DCM approach responds well to the loosely bound induced reactions having contribution of complete fusion (CF) and incomplete fusion (ICF).

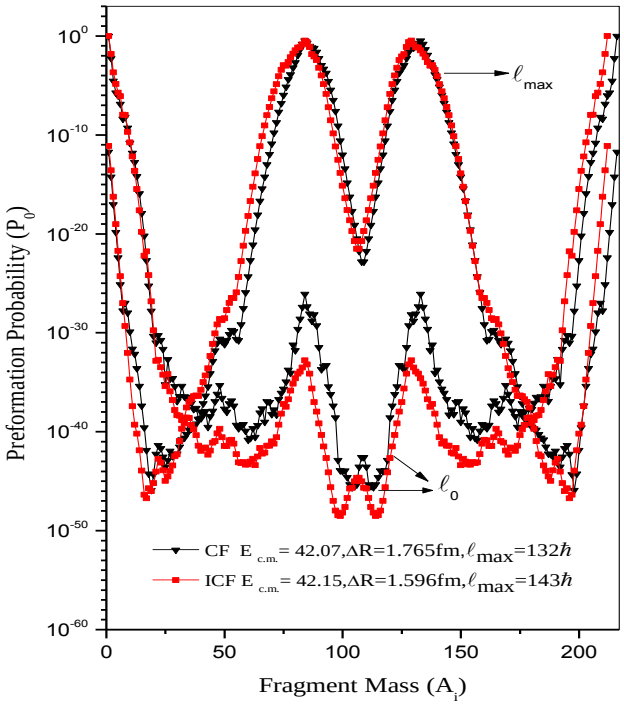

Fig 3.9. *Comparison of CF and ICF based Preformation Probability (P_0) as a function of fragment mass (A_i) for deformed fragmentation at (a)* $E_{c.m.} \cong 42$ MeV

A comparison of fragmentation potential of incomplete fusion (ICF) and complete fusion (CF) is shown in fig. 3.8. From figure, it is detected that, the structure of potential energy surfaces remains same while going from lowest to highest energy in both the processes. However the neck length parameter (ΔR) i.e. the exclusive parameter of DCM, involved in both processes is different and found to decrease as we move from CF to ICF. Further, to explore the difference between CF and ICF

more precisely, we have also plotted the preformation probability (P_0) as a function of fragment mass A_i as shown in fig. 3.9. Figure clearly delineates that, the preformation profile exhibit unambiguous asymmetric distribution for CF as well as ICF processes. Same behaviour is observed at $E_{c.m.}$ = 47.84 MeV (not shown here).

In summary, we have calculated the fragmentation potential for the ER and fission decay channels for compound nuclei $^{217}Rn^{*}$ and $^{218}Fr^{*}$ formed in ^{9}Be + ^{208}Pb and ^{9}Be + ^{209}Bi reactions respectively, for β_2-deformed choice of fragmentation. Potential energy surfaces are almost similar for both decay choices except some arbitrary minima's observed due to the inappropriate deformations associated with some IMF/HMF fragments. Although fission cross-sections are much higher for heavier nucleus, the fragmentation profile looks asymmetric for both the nuclei, independent of decay channel. Moreover, the fragments in the range A_2 = 80-90 seem to contribute towards fission decay for both the reactions. The behaviour of barrier modifications is perused as a function of angular momentum and incident energy. The DCM determined cross sections are in good harmony with experimental data. Following the systematics of neck length parameter (ΔR), ER and fission cross sections are predicted for $^{218}Fr^{*}$ at higher incident energies. At last, the incomplete fusion (ICF) component is addressed in view of loosely bound characteristic of ^{9}Be projectile. Both (CF &ICF) suggest asymmetric fragmentation profile with relatively small neck for the ICF channel. It would be of further heed to address the effect of breakup on fusion data using a miscellany of loosely bound projectiles.

References

[1] M. Dasgupta Phys. Rev. C **81**, 024608 (2010).

[2] R. K. Gupta, M. Balasubramaniam, R. Kumar, D. Singh, C. Beck and W. Greiner, Phys. Rev. C **71**, 014601 (2005).

[3] R. K. Gupta, M. Balasubramaniam, R. Kumar, D. Singh, S. K. Arun and W. Greiner, J. Phys. G: Nucl. Part. Phys. **32**, 345 (2006).

[4] G. Kaur, D. Jain, R. Kumar and M. K. Sharma, Nucl. Phys. A **916** 260 (2013).

[5] G. Sawhney, G. Kaur, M. K. Sharma and R. K. Gupta, Phys. Rev. C **88,** 034603 (2013).

[6] M. Kaur and M. K. Sharma, Eur. Phys. J. A **50** (2014).

[7] K. Sandhu. G. Kaur and M. K. Sharma, Nucl. Phys. A **21,** 114 (2014).

[8] S. K. Arun, R. Kumar and R. K. Gupta, J. Phys. G: Nucl. Part. Phys. **36**, 085105 (2009).

[9] M. K. Sharma, S. Kanwar, G. Sawhney, and R. K. Gupta Phys. Rev. C **85**, 064602 (2012).

[10] M. Dasgupta, P. R. S. Gomes, D. J. Hinde, S. B. Moraes, et al. Phys. Rev. C **70**, 024606 (2004).